Journal of Global Change Data & Discovery. 2026, 10(1): 74-82
www.geodoi.ac.cn

Global Change Research Data Publishing & Repository

Wind Erosion Modulus Dataset Development for the Aral Sea and Surrounding Regions in Central Asia (1990–2020)

YU Yao[1] YAO Feng[2*] LI Changjun[1]

1. Arid Land Ecology and Resources Science Data Center, Xinjiang Institute of Ecology and Geography, Urumqi 830011, China;

2. State Key Laboratory of Ecological Safety and Sustainable Development in Arid Lands, Xinjiang Institute of Ecology and Geography, Urumqi 830011, China

Abstract: The ecological crisis triggered by the shrinkage of the Aral Sea represents a major environmental challenge along the “Belt and Road” route, with soil wind erosion serving as a key process driving salt-dust storms and land degradation. To systematically uncover the long-term evolutionary patterns of soil wind erosion in the Aral Sea region and its surroundings in Central Asia, this study developed an annual wind erosion modulus dataset for the period 1990–2020. This was achieved by integrating multi-source geospatial data on the Google Earth Engine (GEE) platform based on the Revised Wind Erosion Equation (RWEQ). The dataset incorporates MODIS vegetation indices, ESA-CCI land cover data, SRTM elevation data, and ERA5-Land meteorological reanalysis data, which were processed for coordinate system unification, resolution alignment, and spatiotemporal consistency to generate a 31-year sequence of wind erosion modulus at a spatial resolution of 1 km. Data analysis indicates that the dried-up Aral Sea bed is the primary source area for regional wind erosion, with a notable shift in the erosion core from the inner lakebed to its periphery since 2012, reflecting the dynamic evolution of erosion patterns. To validate the reliability of the dataset, simulated results were compared with measured dust flux data recorded at Aral Sea dust monitoring stations (2000–2005) and derived aerosol optical depth (AOD), validating the accuracy and reliability of the dataset in representing wind erosion dynamics in the Aral Sea region. This dataset can serve as a critical data foundation for assessing land degradation, evaluating the effectiveness of ecological restoration projects in the Aral Sea region, and supporting ecological security research for the “Green Silk Road”. Additionally, it provides valuable data support for research and education in geography, ecology, soil and water conservation sciences, and related fields.

Keywords: mulita-source remote; RWEQ model; Aral Sea; interannual variation; Central Asia

DOI: https://doi.org/10.3974/geodp.2026.01.10

Dataset Availability Statement:

Received: 19-10-2025; **Accepted:** 16-01-2026; **Published:** 25-02-2026

Foundations: Department of Science and Technology of Xinjiang Uygur Autonomous Region (2024E02030，PT2406)

***Corresponding Author:** Yao, F., State Key Laboratory of Ecological Safety and Sustainable Development in Arid Lands, Xinjiang Institute of Ecology and Geography, yaofeng@ms.xjb.ac.cn

Data Citation: [1] Yu, Y., Yao, F., Li, C. J. Wind erosion modulus dataset development for the Aral Sea and surrounding regions in Central Asia (1990–2020) [J]. *Journal of Global Change Data* & *Discovery*, 2026, 10(1): 74–82. https://doi.org/10.3974/geodp.2026.01.10.

[2] Yu, Y., Yao, F. Wind erosion modulus dataset for the Aral Sea and surrounding regions in Central Asia (1990–2020) [J/DB/OL]. *Digital Journal of Global Change Data Repository*, 2025. https://doi.org/10.3974/geodb.2025.12.01.V1.

The dataset supporting this paper was published and is accessible through the *Digital Journal of Global Change Data Repository* at: https://doi.org/10.3974/geodb.2025.12.01.V1.

1 Introduction

The Central Asian Aral Sea, located in the hinterland of Eurasia and formerly the world's fourth-largest lake, has become one of the most serious environmental disasters since the 20th century. Since the 1960s, climate change combined with intensive human activities has drastically disrupted the water-resource balance of the Aral Sea Basin. As a result, the lake has continuously shrunk, losing over 90% of its water area by the early 21st century[1,2]. With the large-scale exposure of the lakebed, the regional surface albedo, evapotranspiration pattern, and local climatic conditions have changed significantly, further exacerbating the land degradation process[3,4]. The dried sediments of the former lakebed have become a major source of salt-dust storms and sandstorms. Large quantities of saline dust are transported over long distances by prevailing westerly winds, posing potential ecological threats to northwestern China[3]. The Aral Sea ecological crisis[5–7] is not only a regional challenge in Central Asia, but also a major environmental issue affecting the ecological security pattern of the "Green Silk Road Economic Belt", which has attracted great attention from China and Central Asian countries.

In this context, the Aral Sea region has become a representative area for studying the coupled interactions among land use, hydrology, and climate, as well as their ecological response in arid regions[8]. Since soil wind erosion is a key driving process that triggers the ecological crisis in the Aral Sea, systematically carrying out research on dynamic monitoring and risk assessment of wind erosion in this region is of great practical significance for implementing the China-Central Asia Summit's initiative on "promoting the solution of the ecological crisis in the Aral Sea" and jointly building a China-Central Asia community with a shared future. To support relevant research and decision-making, high-resolution, long-time series soil wind erosion data has become an urgent need. Currently, the combination of remote sensing and wind erosion models has been widely used in regional-scale wind erosion assessment[9–11] among which the revised wind erosion equation (RWEQ) has shown good applicability in arid and semi-arid regions due to its highly accessible parameters and clear physical mechanisms[12]. However, existing data products still have problems of insufficient spatiotemporal resolution or weak validation around the Aral Sea[13].

Based on multi-source remote sensing and reanalysis data, this dataset realizes the regional application and long-term simulation of the RWEQ model on the Google Earth Engine platform, which can be used to analyze the spatiotemporal differentiation law of soil wind erosion during the shrinkage of the Aral Sea[14], identify wind erosion hotspots and evolution trends, and provide key data support for regional land degradation assessment, ecological engineering benefit monitoring[15], and collaborative ecological security governance of the "Belt and Road".

2 Metadata of the Dataset

The metadata of the Wind erosion modulus dataset for the Aral Sea and surrounding regions in Central Asia (1990–2020)[16] is summarized in Table 1. It includes the dataset full name, short name, authors, year of the dataset, temporal resolution, spatial resolution, data format, data size, data files, data publisher, and data sharing policy, etc.

Table 1 Metadata summary of the Wind erosion modulus dataset for the Aral Sea and surrounding regions in Central Asia (1990–2020)

Items	Description
Dataset full name	Wind erosion modulus dataset for the Aral Sea and surrounding regions in Central Asia (1990–2020)
Dataset short name	AralSea_WEMD_1990-2020
Authors	Yu, Y., Xinjiang Institute of Ecology and Geography, Arid Land Ecology and Resources Science Data Center, yuyao@ms.xjb.ac.cn Yao, F., Xinjiang Institute of Ecology and Geography, State Key Laboratory of Ecological Safety and Sustainable Development in Arid Lands, yaofeng@ms.xjb.ac.cn
Geographical region	Aral Sea Basin (44°N–47°N, 58°E–62°E)
Year	1990–2020
Temporal resolution	Year
Spatial resolution	1 km
Data format	.tif
Data size	260 MB
Data files	Wind erosion modulus data for the Aral Sea and surrounding regions in Central Asia
Foundations	Department of Science and Technology of Xinjiang Uygur Autonomous Region (2024E02030，PT2406)
Data publisher	Global Change Research Data Publishing & Repository, http://www.geodoi.ac.cn
Address	No. 11A, Datun Road, Chaoyang District, Beijing 100101, China
Data sharing policy	(1) *Data* are openly available and can be free downloaded via the Internet; (2) End users are encouraged to use *Data* subject to citation; (3) Users, who are by definition also value-added service providers, are welcome to redistribute *Data* subject to written permission from the GCdataPR Editorial Office and the issuance of a *Data* redistribution license; and (4) If *Data* are used to compile new datasets, the “ten percent principal” should be followed such that *Data* records utilized should not surpass 10% of the new dataset contents, while sources should be clearly noted in suitable places in the new dataset[17]
Communication and searchable system	DOI, CSTR, Crossref, DCI, CSCD, CNKI, SciEngine, WDS, GEOSS, PubScholar, CKRSC

3 Methods

This dataset integrates multi-source remote sensing, reanalysis and observation data to drive the calculation and validation of wind erosion modulus in the study area. The data used are summarized in Table 2.

Table 2 Data sources

No.	Data type	Data source	Data content	Spatial resolution	Time range
1	Ground observation	NOAA	Meteorological station data (wind speed, etc.)	–	1990–2023
2	Meteorological data	ECMWF ERA5-Land	Wind speed, temperature, precipitation, snow depth	1 km	1990–2023
3	Remote sensing	MODIS	Land surface temperature, vegetation cover, aerosol optical depth	1 km	1990–2023
4	Land cover data	ESA CCI	Global land-cover data	300 m	1990–2023
5	Topographic data	SRTM	Elevation data	30 m	–
6	Soil data	HWSD	Soil properties (texture, organic matter, etc.)	1 km	–
7	Field sampling	Kazakhstan Aral Sea dry lakebed	Soil sampling data (29 sites)	–	June 2018
8	Dust/salt monitoring	Aral Sea Dust Monitoring Stations	Dust/salt deposition data	–	2000–2005

3.1 Data Preprocessing

This dataset uses the ERA5-Land reanalysis dataset[1] released by the European Centre for Medium-Range Weather Forecasts (ECMWF) as the primary meteorological data source. The dataset provides hourly estimates of near-surface wind speed, temperature, and precipitation with a spatial resolution of 0.1° (approximately 10 km). To improve the reliability of wind speed inputs, daily observational records from NOAA[2] (National Oceanic and Atmospheric Administration) ground stations in the study area were incorporated, and a quantile mapping method was applied to systematically correct biases in the ERA5 Land wind speed data. Validation shows that the corrected data align well with measured values, with a coefficient of determination (R^2) exceeding 0.87.

The remote sensing dataset forms the core of spatial analysis. This dataset extracts 1-km spatial resolution normalized difference vegetation index (NDVI), aerosol optical depth (AOD), and land surface temperature (LST) from Moderate Resolution Imaging Spectroradiometer (MODIS) data. The vegetation index was derived from the MOD13A2 product[3] (U.S. Geological Survey/NASA) and undergoes Z-score standardization to reduce sensor-specific biases. Land cover data is obtained from the European Space Agency's Climate Change Initiative project's 300-m resolution dataset[4] and aggregated to 1-km resolution using a majority resampling method. Topographic data[5] was acquired from the Shuttle Radar Topography Mission (SRTM) at a 30-m resolution and upscaled to 1 km using a mean resampling method to match other data sources.

To ensure temporal consistency and interannual comparability, all datasets were projected to the WGS 1984 geographic coordinate system and resampled to a consistent 1-km spatial resolution using bilinear interpolation (for continuous variables) and nearest neighbor method (for categorical data). For NDVI, AOD, and precipitation data, a five-year moving-average filter was applied for temporal smoothing to effectively suppress short-term anomalies and sensor noise.

The soil attribute information was extracted from the Harmonized World Soil Database[6] with a spatial resolution of 1 km, including key parameters such as soil texture, organic matter content, and calcium carbonate content, which are core inputs for calculating the soil erodibility factor in the RWEQ model. Through validation of data from 29 field sampling points, the errors in soil parameters were well controlled within acceptable limits (texture ±5%, organic matter ±0.5%).

3.2 The Revised Wind Erosion Equation Model

The Revised Wind Erosion Equation (RWEQ) is an erosion estimation model developed based on empirical methods. Its core mechanism lies in comprehensively simulating the combined effects of multiple factors on the wind erosion process, such as climate (e.g., wind speed, precipitation), soil (e.g., erodibility component content), and surface cover (e.g., vegetation, roughness). It has become a widely used tool for quantifying the intensity of soil wind erosion in arid and semi-arid regions[18–20].

In this study, the key input parameters of the RWEQ model were derived from remote sensing and meteorological datasets. The wind erosion rate per unit area is calculated as follows:

---

[1] ERA5-Land. https://cds.climate.copernicus.eu/datasets/reanalysis-era5-land?tab=documentation.

[2] NOAA daily observational data. https://www.ncei.noaa.gov/data/global-summary-of-the-day/archive/.

[3] MOD13A2. https://ladsweb.modaps.eosdis.nasa.gov/.

[4] SA CCI. https://maps.elie.ucl.ac.be/CCI/viewer/.

[5] SRTM. https://dwtkns.com/srtm30m/.

[6] HWSD. https://gaez.fao.org/pages/hwsd.

$$Q_R = \frac{2z}{S^2} Q_{max} e^{-\left(\frac{z}{s}\right)^2} \tag{1}$$

$$S = 150.71(WF \times EF \times SCF \times K' \times C)^{-0.3711} \tag{2}$$

$$Q_{max} = 109.8(WF \times EF \times SCF \times K' \times C) \tag{3}$$

where Q_R is the soil erosion rate (t/(hm^2·a)), Q_{max} is the maximum soil transport rate (kg/m), and z is the distance downwind where maximum erosion occurs (m). The model assumes that maximum wind erosion occurs at the midpoint of the field ($z \approx S/2$), and S is the plot length (m), WF is the climatic factor, EF is the soil erodibility factor, SCF is the soil crust factor, K' is the surface roughness factor, C is the vegetation cover factor.

The climatic factor (WF) is calculated as:

$$WF = \frac{SW \times SD \times \sum_{i=1}^{N} u_2 (u_2 - u_1)^2 \times \frac{\rho}{g} \times N_d}{500} \tag{4}$$

where SW represents soil moisture (%), SD denotes the snow cover factor, u_2 indicates measured wind speed at 2 m (m/s), u_1 is the threshold wind speed at 2 m (assumed 5 m/s) ($u_2 > u_1$), N is the number of wind-speed-observation periods, N_d refers to the number of days (d), ρ is the air density (kg/m^3), and g represents gravitational acceleration (m/s^2).

The soil erodibility factor (EF) and soil crust factor (SCF) are calculated as:

$$EF = \frac{29.09 + 0.31 + SA + 0.17 \times SI + 0.33 \times \frac{SA}{CL} - 2.59 \times OM - 0.95 \times CaCO_3}{100} \tag{5}$$

$$SCF = \frac{1}{1 + 0.0066 \times CL^2 + 0.021 \times OM^{2'}} \tag{6}$$

where SA, CL, and SI denote the percentages of sand, clay, and silt, respectively (%), OM represents the soil organic matter content (%), and $CaCO_3$ represents the calcium carbonate content (%). The vegetation cover factor (C) is calculated for 5 land cover types (forest, shrubland, grassland, cropland, and bare land) using the following Equation:

$$C = e^{a_i (SC)} \tag{7}$$

where a_i is a vegetation-specific coefficient, and SC denotes the vegetation cover derived from NDVI (%). These vegetation-specific coefficients a_i were adopted from Fryrear[21] for arid environments, with values of 0.153,5 (forest), 0.092,1 (shrubland), 0.151,1 (grassland), 0.043,8 (cropland), and 0.076,8 (bare land), consistent with the land cover types in the study area.

3.3 Google Earth Engine Platform Computation

Google Earth Engine (GEE) was used as the computational platform for this study. Its unique cloud-based architecture effectively addresses 3 key challenges in large-scale wind erosion simulation. First, the GEE's built-in parallel computing capability supports efficient processing of 31 years of temporal data (1990–2020) for the Aral Sea region. Second, the platform integrates multi-source geospatial datasets, including MODIS surface reflectance products, ERA5-Land meteorological reanalysis data, and SRTM elevation data, enabling seamless data access and unified management. Third, its optimized spatial analysis functions ensure the feasibility of regional-scale simulations while maintaining pixel-level computational accuracy at a 1-km resolution. The integrated framework of GEE demonstrates exceptional computational efficiency, requiring only 1 day to fully generate a 31-year annual spatial dataset of wind erosion modulus, providing critical technical support for long-term, large-scale wind erosion simulation studies.

The technical workflow of this study is illustrated in Figure 1. This computational framework consists of 3 main steps. First, during the data preprocessing stage, meteorological datasets (ERA5, NOAA) and land cover datasets (MODIS, ESACCI) were resampled to a 1-km resolution to ensure spatial consistency, and wind speed data were corrected using bias adjustment techniques to improve accuracy. Second, the RWEQ model was applied to calculate the spatiotemporal distribution of wind erosion rates from 1990 to 2020. Finally, the optimized model was used to simulate monthly-scale soil wind erosion potential in the Aral Sea Basin from 1990 to 2020, generating a continuous spatiotemporal dataset. The simulated erosion rates were subsequently validated and calibrated using dust flux observations and satellite-derived aerosol optical depth (AOD) data.

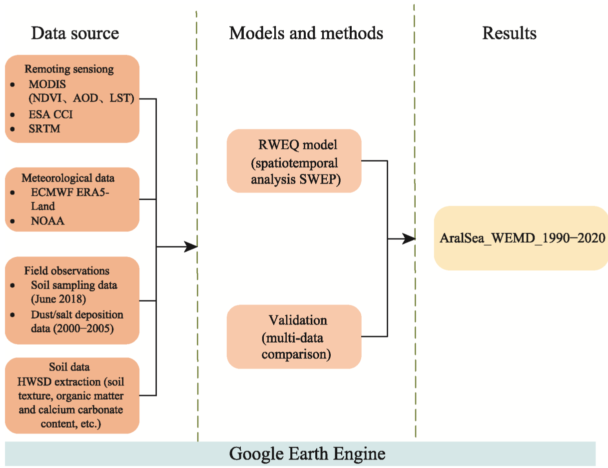

Figure 1 Flowchart of the dataset development

4 Data Results and Validation

4.1 Dataset Composition

The dataset of wind erosion modulus for the Aral Sea region and surrounding areas in Central Asia contains 31 spatial datasets of soil wind erosion modulus from 1990 to 2020. All data are archived in .tif format at a spatial resolution of 1 km, with pixel values expressed in kg/m^2/y. The naming convention for the data files follows: ASSR-WEMD-Year.tif, where ASSR stands for “Aral Sea and Surrounding Regions”, WEMD represents “Wind Erosion Modulus Dataset”, and Year represents the four-digit year. For example, ASSR-WEMD-2010.tif represents the raster data of soil wind erosion modulus for the year 2010 in this region.

All layers in this dataset share a unified geographic coordinate system and pixel size, facilitating time-series analysis and spatial modeling. Each .tif file contains a single-band floating-point raster layer, where the pixel value indicates the average annual wind erosion modulus at that location. To illustrate the dataset’s characteristic temporal patterns, 3 representative years are selected for explanation: (1) ASSR-WEMD-2005.tif, the year with the lowest wind erosion modulus, reflecting the weakening phase of wind erosion activity from the early to mid-period. (2) ASSR-WEMD-2010.tif, a critical transitional year when wind erosion modulus exhibited a significant increase. (3) ASSR-WEMD-2015.tif, the year with the peak wind erosion modulus in the entire time series, marking the phase of highest erosion intensity.

4.2 Data Results

Figure 2 illustrates the spatial distribution of wind erosion modulus across 31 annual layers from 1990 to 2020. In terms of overall interannual variation, the Aral Sea Basin, particularly its eastern dried-up lakebed area, consistently remained the core region of erosion, with the intensity generally showing an increasing trend. Notably, beginning around 2012, erosion within the lakebed weakened, while erosion intensity in the surrounding areas notably intensified. This indicates that the erosion extent is expanding and that the primary erosion source has gradually shifted from the exposed central lakebed to the vegetation degraded, soil-fragile coastal regions and adjacent regions.

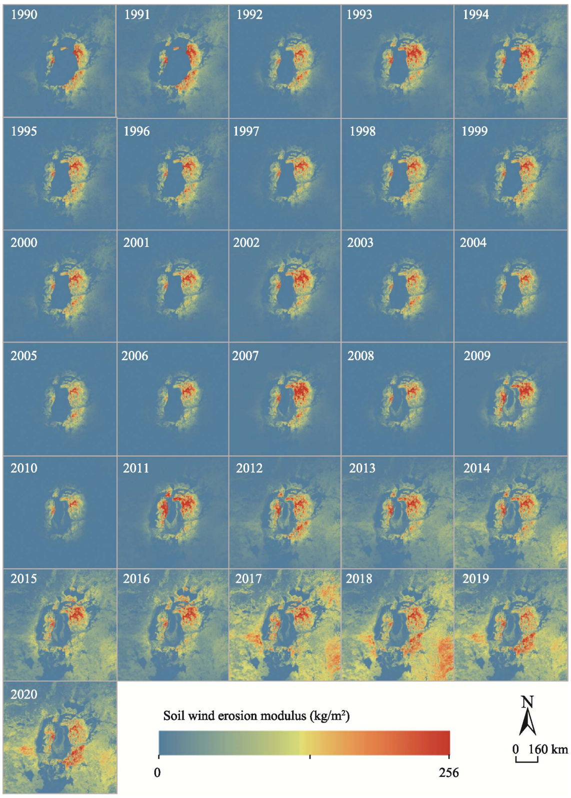

Figure 2 Interannual spatial distribution maps of soil wind erosion model (1990–2020)

Over the entire study period from 1990 to 2020, the regional soil wind erosion modulus exhibited a significant mean annual increase of 0.33 kg/m^2, with spatial variability ranging from –1.2 to 5.09 kg/m^2. Among these, areas experiencing severe intensification of wind erosion (annual growth rate>1.8 kg/m^2) were primarily concentrated in 3 types of regions: the newly dried-up central lakebed of the Aral Sea, the active sandy areas of the Kyzylkum Desert, and the fragile surface regions of the western plateau. These regions share common characteristics such as loose surface material and extremely low vegetation coverage, making them highly sensitive to wind disturbance and environmental changes. In contrast, surrounding around the remaining water bodies in the northern Aral Sea and the irrigated oasis zones in the lower deltas of the Syr Darya and Amu Darya rivers exhibited minimal annual change rates (<0.1 kg/m^2). This is primarily attributed to the relatively stable vegetation cover maintained by water bodies or irrigation, which effectively suppresses wind erosion development.

4.3 Data Validation

To assess the accuracy and reliability of the annual spatial dataset of wind erosion modulus for the Aral Sea region in Central Asia from 1990 to 2020, this study employed a multi-source cross-validation approach to systematically compare the consistency between simulation results and independent observational datasets.

First, the measured dust flux data recorded by monitoring stations in the Aral Sea region (2000–2005) were compared with simulated wind erosion modulus values at corresponding locations. The results indicate a high degree of consistency in spatial patterns between the two, with a strong correlation (r=0.72, p<0.05), demonstrating that the model can reliably capture the spatiotemporal variation characteristics of regional wind erosion. Furthermore, a regional correlation analysis was conducted between the simulated annual wind erosion modulus and satellite-derived aerosol optical depth (AOD). The analysis revealed a highly significant interannual correlation (r=0.85, p<0.001), indicating strong consistency between the simulation outputs and remote-sensing indicators of atmospheric dust load. Together, this multi-source evidence collectively validates the accuracy and reliability of the dataset in representing wind erosion dynamics in the Aral Sea region.

5 Discussion and Conclusion

This dataset is archived in .tif format and can be directly read, visualized, spatially queried, statistically analyzed, and mapped using mainstream geographic information and remote-sensing platforms such as ArcGIS, QGIS, ENVI, and Google Earth Engine. It is well suited for analyzing interannual trends in soil wind erosion modulus, identifying spatiotemporal pattern evolution, and studying driving mechanisms in the Aral Sea region from 1990 to 2020. It can also serve as foundational data for wind erosion risk assessment, land degradation monitoring, and evaluations of ecological governance effectiveness. Additionally, this dataset can be used as input data for future wind erosion scenario simulations, providing scientific support for ecological restoration and regional sustainable development decision-making in the Aral Sea region.

This study also highlights several areas for future improvement and refinement. (1) Optimization of models and input data: The current model primarily relies on satellite remote sensing and reanalysis data. Future work could incorporate higher spatiotemporal resolution remote sensing products (e.g., Sentinel series data) and incorporate key parameters such as field-measured wind speed and soil properties to further enhance the model’s simulation accuracy, particularly in characterizing local microtopography and soil heterogeneity. (2) Refinement of process-based mechanisms: The existing framework is mainly based on the RWEQ for interannual-scale simulations. Future research could incorporate more complex wind erosion process models or couple hydrological and vegetation dynamics models to more finely capture daily/ seasonal-scale wind erosion events, the effects of soil moisture and freeze-thaw cycles, and the feedback mechanisms between vegetation dynamics and wind erosion processes. (3) Expansion of application scenarios and decision support potential: Future studies could combine this dataset with regional climate models and land-use change scenarios to conduct high-resolution wind erosion risk prediction and early warning research. Additionally, efforts could be made to integrate wind erosion modulus data with ecosystem service assessment models and socioeconomic data to quantify the economic and social impacts of wind erosion disasters, thereby providing stronger decision support for formulating more targeted ecological restoration and adaptive management strategies.

Through continuous improvements in these areas, future work is expected to further deepen our understanding of wind-erosion processes in the Aral Sea region and to provide more precise, forward-looking assessment tools and data foundations for other wind-erosion-prone arid and semi-arid regions worldwide.

Author Contributions

Yu, Y. handled data statistics and authored the data paper; Yao, F. oversaw the overall design of the dataset development, data quality control, and paper revisions; Li, C. J. contributed to the data validation.

Conflicts of Interest

The authors declare no conflicts of interest.

References

[1] Micklin, P. The past, present, and future Aral Sea [J]. *Lakes* & *Reservoirs*: *Research* & *Management*, 2010, 15(3): 193–213.

[2] Gaybullaev, B., Chen, S. C., Kuo, Y. M. Large-scale desiccation of the Aral Sea due to over-exploitation after 1960 [J]. *Journal of Mountain Science*, 2012, 9: 538–546.

[3] Indoitu, R., Orlovsky, N., Orlovsky, L. Dust emission and environmental changes in the dried bottom of the Aral Sea [J]. *Aeolian Research*, 2015, 17: 101–115.

[4] Shibuo, Y., Jarsjö, J., Destouni, G. Hydrological responses to climate change and irrigation in the Aral Sea drainage basin [J]. *Geophysical Research Letters*, 2007, 34(21): L21406.

[5] He, M. Z., Gao, X., Zhao, Z. Y., *el al*. The ecological crisis of the Aral Sea: desertification trends and ecological restoration and prevention strategies [J]. *Bulletin of the Chinese Academy of Sciences*, 2021, 36(2): 130–140.

[6] Deng, M. J., Long, A. H. Analysis of hydrological and water resource evolution in the Aral Sea Basin and solutions to the Aral Sea ecological crisis [J]. *Glaciers and Frozen Soil*, 2011, 33(6): 1363–1375.

[7] Destouni, G., Jaramillo, F., Prieto, C. Hydroclimatic shifts driven by human water use for food and energy production [J]. *Nature Climate Change*, 2013(3): 213–217.

[8] Kristopher, D. W. Nature-society linkages in the Aral Sea region [J]. *Journal of Eurasian Studies*, 2013, 4(1): 18–33.

[9] Lesimuchu. Assessment of soil wind erosion and research on windbreak and sand fixation service flows in Northwest China, 1980–2015 [D]. Xi'an: Chang'an University, 2019.

[10] Zhang, Q. Q., Gu, F., Zhang, S. C., *et al*. Spatiotemporal variation in wind erosion in Tarim River Basin from 2010 to 2018 [J]. *Land*, 2024, 13(3): 330.

[11] Jiang, H. T., Gao, W. B., Liu, B. Y., *et al*. Quantifying soil wind erosion attribution in Inner Mongolia's desert grassland [J]. *Scientific Reports*, 2025(15): 14319.

[12] Borrelli, P., Robinson, D. A., Panagos, P., *et al*. Land use and climate change impacts on global soil erosion by water (2015–2070) [J]. *Proceedings of the National Academy of Sciences of the United States of America*, 2020, 117(36): 21994–22001.

[13] Jiang, L. L., Jiapaer, G., Bao, A. M., *et al*. Monitoring the long-term desertification process and assessing the relative roles of its drivers in Central Asia [J]. *Ecological Indicators*, 2019, 104: 195–208.

[14] Lin, J. K. Spatio-temporal variation of soil erosion and its driving factors in the Hexi Corridor [D]. Lanzhou: Lanzhou University, 2020.

[15] Li, J. Y., Yang, X. C., Jin, Y. X., *et al*. Monitoring and analysis of grassland desertification dynamics using Landsat images in Ningxia [J]. *Remote Sensing of Environment*, 2013, 138: 19–26.

[16] Yu, Y., Yao, F. Wind erosion modulus dataset for the Aral Sea and surrounding regions in Central Asia (1990–2020) [J/DB/OL]. *Digital Journal of Global Change Data Repository*, 2025. https://doi.org/10.3974/geodb.2025.12.01.V1.

[17] GCdataPR Editorial Office. GCdataPR data sharing policy [OL]. DOI: 10.3974/dp.policy.2014.05 (Updated in 2017).

[18] Evans, J., Geerken, R. Discrimination between climate and human-induced dryland degradation [J]. *Journal of Arid Environments*, 2004, 57(4): 535–554.

[19] Chen, Z., Liu, J. Y., Hou, X. T., *et al*. Detection and attribution of greening and land degradation of dryland areas in China and America [J]. *Remote Sensing*, 2023, 15(10): 2688.

[20] Borrelli, P., Lugato, E., Montanarella, L., *et al*. A new assessment of soil loss due to wind erosion in European agricultural soils using a quantitative spatially distributed modelling approach [J]. *Land Degradation* & *Development*, 2017, 28(1): 335–344.

[21] Fryrcar, D. W., Chen, W. N., Lester, C. Revised wind erosion equation [J]. *Annals of Arid Zone*, 2001, 40(3): 265–279.